

InP/GaAsSb/InP DHBT: Analysis of specific material parameters and high current effect by physical simulation

C. Maneux¹, M. Belhaj¹, N. Labat¹, A. Touboul¹, M. Riet², M. Kahn², J. Godin², Ph. Bove³

¹ IXL, CNRS, Université Bordeaux 1, 351 Cours de la Libération, 33405 Talence, France, Phone: +33 5 4000 28 58

² ALCATEL R&I - OPTO+, Route de Nozay, 91461 Marcoussis Cedex, France, Phone: +33 1 69 63 46 93

³ PICOGIGA International S.A.S., Place Marcel Rebuffat, 91971 Courtaboeuf, France, Phone: +33 1 69 31 61 30

Abstract — Although InP/GaAs_{0.51}Sb_{0.49}/InP DHBT has recently attracted much interest, some sensitive material parameters are still uncertain. We detailed the simulation methodology used to evaluate bandgap energy, minority carrier lifetime and band gap narrowing effect. Moreover, the high-injection effect is analysed as resulting from electron parasitic barrier formation at base-collector junction.

I. INTRODUCTION

The InP/GaAsSb/InP DHBT have recently attracted much interest, mainly owing to GaAsSb/InP type II heterojunction which favours the injection of electrons from the base into the collector. Since the development of the first InP/GaAsSb/InP HBT [1,2], various doping and structure designs have been performed [3,4] to improve both ac and dc performances. Accurate physical simulation can save expensive technological effort to obtain significant improvements of the device performances. However, to authors knowledge, simulation of InP/GaAsSb/InP HBT has still not been reported. This is probably due to lack of experimental results and data regarding the material characteristics of the p-type carbon highly doped GaAs_{0.51}Sb_{0.49} base. As one of the key points to construct trustful simulation is the accuracy of material parameters, this paper presents 2D simulation of dc characteristics of InP/GaAsSb/InP DHBT with the procedure developed to adjust unknown material parameters. The comparison between measured dc characteristics and simulated ones is used to validate this study.

II. SIMULATION

A schematic view of DHBT cross-section and a description of the epilayers are given respectively in figure 1 and table 1. Using the symmetry properties of the structure, it is possible to limit the simulation domain to half a device (a symmetry axis is considered in the middle of emitter). The virtual device is built with the solid modeller MDRAW-ISE. DESSIS-ISE software is used to simulate the DHBT dc characteristics. The carrier transport mechanisms are described by hydrodynamic model derived from Stratton energy balance equations [5]. To take into account high doping effect in the GaAsSb base layer, Fermi-Dirac statistics and bandgap narrowing are considered.

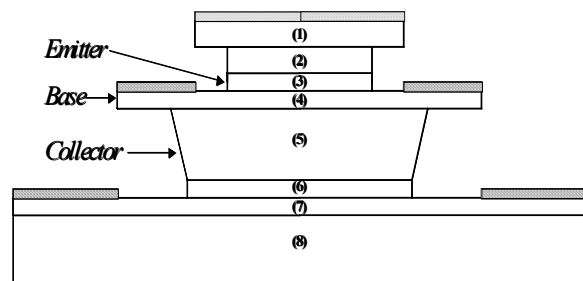


Fig. 1. Schematic view of the cross-section of the simulated DHBT and description of its epitaxial structure. The emitter surface is $(3 \times 20) \mu\text{m}^2$.

Layer	Doping (cm^{-3})	Thickness (nm)
(1) InGa _{0.47} As _{0.53}	(Si) 1×10^{19}	100
(2) n ⁺⁺ InP	(Si) 3×10^{19}	100
(3) n ⁺ InP	(Si) 3×10^{17}	50
(4) p GaAs _{0.51} Sb _{0.49}	(C) 4×10^{19}	50
(5) n InP	(Si) 1×10^{16}	300
(6) n ⁺⁺ InP	(Si) 1×10^{19}	50
(7) InGa _{0.47} As _{0.53}	(Si) 1×10^{19}	50
(8) InP (semi-insulator)	(Fe) -	-

Table 1: Description of the DHBT epitaxial layers

III. RESULTS

A. Band Gap Narrowing of GaAsSb base layer

The theoretical value [6], $E_G^{th} = 0.72$ eV of the energy band gap of GaAs_{0.49}Sb_{0.51} at 300K does not account for effects of possible (i) strain and ordering known to result in overall reduction of the band gap energy or (ii) band gap energy reduction due to the heavy doping. Hence, base energy band gap, $E_{GB} = E_G^{th} - \Delta E_G$ is introduced in the simulation where ΔE_G is the band gap narrowing (BGN). The band gap narrowing results in the lowering of the conduction band δ_C and/or the upward shift of the valence band δ_V , such that $\delta_V + \delta_C = \Delta E_G$ as it is sketched in figure 2.

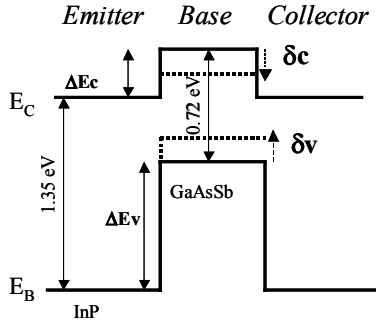


Fig. 2. Schematic illustration of the band gap lineup in the intrinsic DHBT

As, the ΔE_G distribution between the conduction and the valence energy bands has not significant effect on the DHBT dc curves [7], ΔE_G is assumed to be equally distributed between the valence and conduction energy bands ($\delta_V = \Delta E_G/2$ and $\delta_C = \Delta E_G/2$). To determine ΔE_G , the collector current density, J_C , is simulated under forward bias for different ΔE_G values (0 to 105 meV). Figure 3 shows the comparison between measured and simulated collector current density, J_C . The best agreement is achieved for $\Delta E_G = 70$ meV.

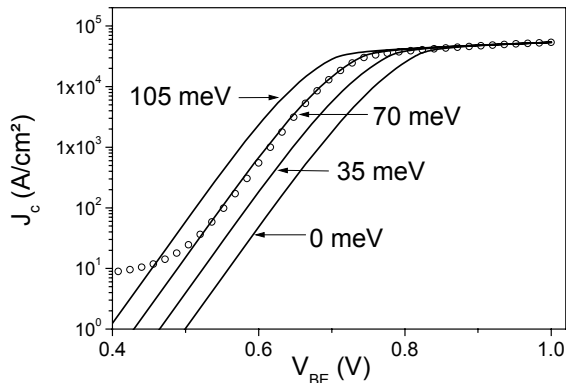


Fig. 3. Measured (O) and simulated (solid line) collector current density as function of base-emitter bias for $V_{CB}=0$ V and for ΔE_G (BGN) values of 0, 35, 70 and 105 meV

B. GaAs Minority Carrier Lifetime

Assuming that radiative recombinations are always negligible at high doping level and according to references [8,9], Auger, radiative and surface SRH recombination mechanisms are ignored, only SRH bulk recombinations into the p-GaAsSb base are considered. To estimate the minority carrier life time, τ_n , forward Gummel characteristics were simulated for different τ_n values and compared to the measured one. In these simulations, the GaAsSb recombination centers are assumed to be located at mid gap. Simulated and measured Gummel plots are shown in figure 4. and show good agreement for $\tau_n \approx 0.5$ ns.

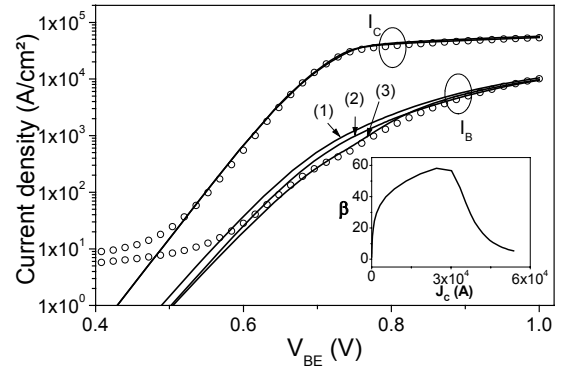


Fig. 4. Measured (O) and simulated base and collector currents densities versus base-emitter bias for $V_{CB}=0$ V and for three values of electron life-time in the base: $\tau_n = 0.05$ ns (1), $\tau_n = 0.25$ ns (2) and $\tau_n = 0.5$ ns (3)

C. High Current Effect

The purpose is to investigate the mechanism responsible for the gain drop at high J_C observed in the inset of figure 4 for collector current density, J_C higher than 3×10^4 A/cm² (V_{BE} around 0.73 V). Indeed, At low injection currents, $J_C < 3 \times 10^4$ A/cm², the electron density in the collector (figure 5b) is smaller than the donor concentration in the lightly doped collector (10^{16} cm⁻³). The electric field, in the C-B space charge region has the expected triangular shape with a maximum negative value close to the B-C interface (figure 5a). When J_C reaches 30 kA/cm², the density of electrons into the collector starts to exceed the collector donor doping concentration and corresponds to the onset of the high injection regime. In homojunction bipolar devices, to compensate the excess electron concentration, holes are injected from the base to the collector leading to the well known base push-out effect (Kirk effect). However, for the InP/GaAsSb heterojunction, no classical base push-out can take place in the InP/GaAsSb system, because the large valence band discontinuity at the B-C heterointerface, ΔE_V (0.88 eV) opposes the flow of holes from the base to the collector. Indeed, even at J_C values higher than 30 kA/cm², the hole density into the collector remains much lower than the electron density.

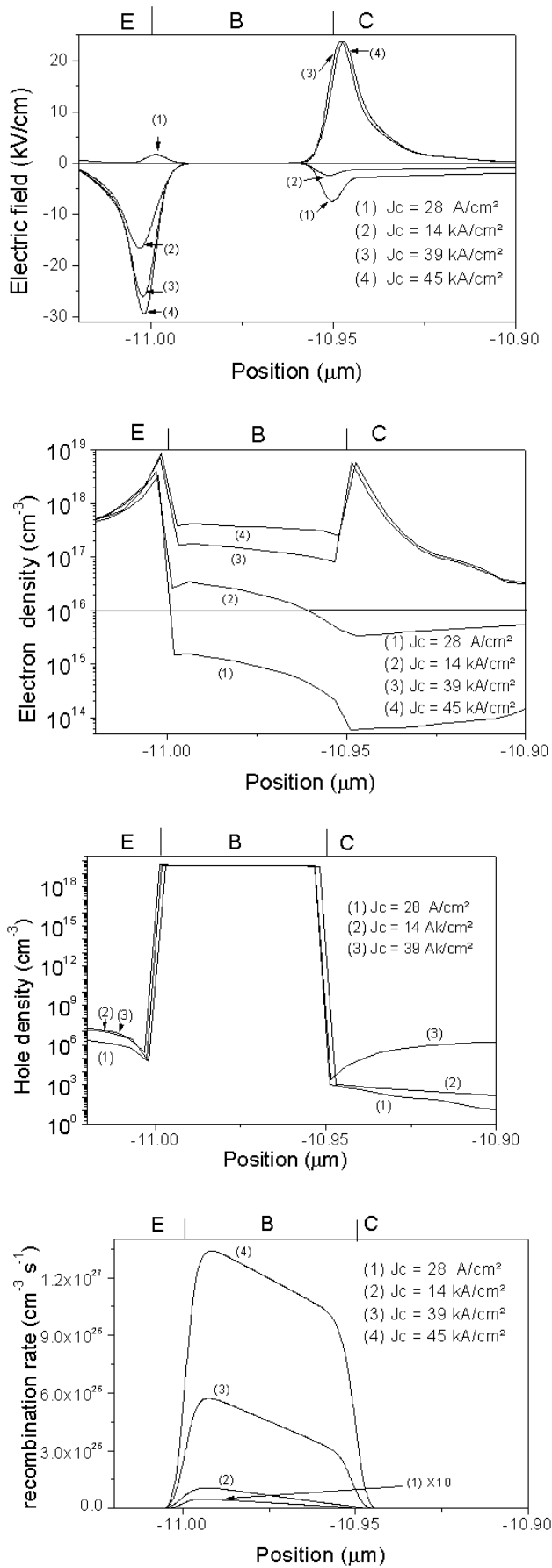


Fig. 5. Profile of :
 Electric field Electron density
 Hole density Electron-hole recombination rate
 at $V_{BE}=0 \text{ V}$ and for four collector current densities

Instead of the occurrence of the classical base push-out effect, a parasitic electron barrier build up at the base-collector interface [10]. The positive, electric field spike near the base-collector junction in figure 4a, corresponds to a potential barrier. This positive retarding electric field has two effects on the dc operation of the DHBT:

- (i) Many of electrons injected to the collector are reflected back at the B-C heterojunction, leading to the quasi-saturation of J_C observed around $V_{BE}=0.73 \text{ V}$ in figure 4 and hence, the increase of the electron density into the base.
- (ii) Holes are injected into the base to ensure the charge quasi-neutrality. This effect causes an increase of the electron-hole recombination rate into the base (figure 5d) and hence the rise of the base current, J_B , is observed in figure 4, at $V_{BE}=0.73 \text{ V}$.

The resulting increase in the base current together with the saturation of the collector current cause the abrupt decrease of current gain for $J_C > 3 \times 10^4 \text{ A/cm}^2$.

Figures 6 and 7 summarize the impact of either intrinsic (donor concentration and depth) and extrinsic (ohmic contact resistivity) DHBT collector parameters on the onset of high current effect regarding the evolution of gain current versus collector current density.

Indeed, it is important to understand the dependence of the parasitic barrier formation at the base-collector interface on device features. Obviously, higher is the onset of the parasitic barrier formation, J_{CK} , better the DHBT dc and ac performances at high collector current density. Therefore, we have studied the dependence of J_{CK} , as a function of intrinsic and extrinsic device structure parameters as well collector thickness and doping concentration as collector ohmic contact resistivity.

The onset of the electron parasitic barrier formation, at $V_{BC}=0 \text{ V}$, is commonly expressed as:

$$J_{CK} = qv_{sat} \left(N_C + \frac{2\varepsilon V_{bi}}{qW_C^2} \right) \quad (1)$$

Where v_{sat} is the electron saturation velocity into InP collector ($1.2 \times 10^7 \text{ cm/s}$), V_{bi} is the base-collector built-in potential, ε is the InP static dielectric permittivity, N_C , the collector doping concentration and W_C the collector thickness.

According to Eq. (1), reducing W_C from 300 nm to 200 nm and increasing N_C from $1 \times 10^{16} \text{ cm}^{-3}$ to $5 \times 10^{16} \text{ cm}^{-3}$, should approximately multiply J_{CK} by four. The comparison between the simulated current gain for two sets of collector parameters, $N_C=1 \times 10^{16} \text{ cm}^{-3}$, $W_C=300 \text{ nm}$ and $N_C=5 \times 10^{16} \text{ cm}^{-3}$, $W_C=200 \text{ nm}$ is shown in figure 6. Contrary to the results expected from equation 1, no more than 10% rise of J_{CK} is observed.

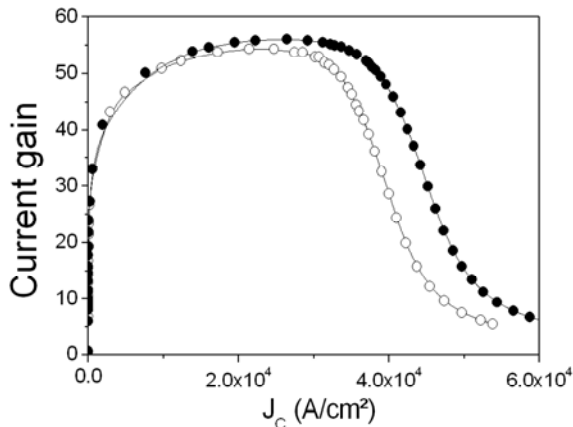


Fig. 6. Simulated current gain versus collector current density at $V_{BC} = 0$ V for two collector structure configurations with collector contact resistivity of $4 \times 10^{-6} \Omega \text{cm}^2$:
 (o) $N_C = 1 \times 10^{16} \text{ cm}^{-3}$ and $W_C = 300$ nm,
 (•) $N_C = 5 \times 10^{16} \text{ cm}^{-3}$ and $W_C = 200$ nm.

Figure 7 shows the simulated current gain as a function of the collector current density for different values of collector contact resistivity, ρ_C . Both simulation fitting procedure and measurements on TLM test structures have lead to $4 \times 10^{-6} \Omega \text{cm}^2$ collector ohmic contact resistivity. The decrease of ρ_C , greatly increases the DHBT current gain at high collector current density. Indeed, J_{CK} rises from $3 \times 10^4 \text{ A/cm}^2$ to more than $3 \times 10^5 \text{ A/cm}^2$ when ρ_C is decreased from $4 \times 10^{-6} \Omega \text{cm}^2$ to $4 \times 10^{-7} \Omega \text{cm}^2$. In complement to Eq. (1) defining a J_{CK} threshold related to intrinsic operation, the results presented here emphasize the importance of the collector ohmic contact resistivity to improve HBT performances at high collector current density.

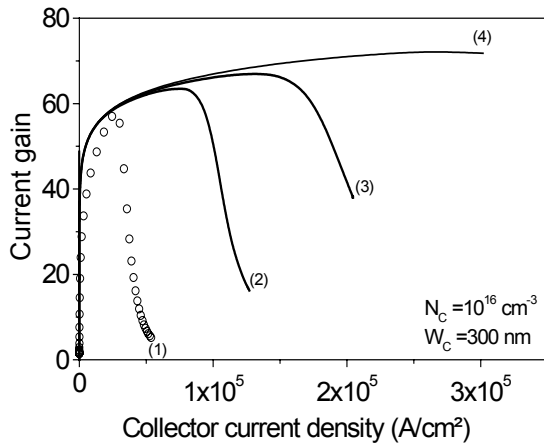


Fig. 7. Simulated current gain versus collector current density at $V_{BC} = 0$ V for collector ohmic contact resistivity of:
 (1) $\rho_C = 4 \times 10^{-6} \Omega \text{cm}^2$; (2) $\rho_C = 1 \times 10^{-6} \Omega \text{cm}^2$
 (3) $\rho_C = 2 \times 10^{-6} \Omega \text{cm}^2$; (4) $\rho_C = 4 \times 10^{-7} \Omega \text{cm}^2$
 The collector doping is 10^{16} cm^{-3} and its depth is 300 nm.

In fact, the well-known relation (Eq.(1)) used to evaluate J_{CK} , does not take into account an extrinsic parasitic effect, which is the collector voltage drop due to the sub-collector ohmic contact resistivity and hence overestimates the impact of the intrinsic collector parameters, N_C and W_C , on J_{CK} .

The reduction of the sub-collector contact resistivity does not eliminate the mechanisms leading to the formation of the parasitic barrier, but notably shifts its effect on the current gain to higher collector current density. Thus, the enhancement of the DHBT operation at high current density requires not only the optimisation of intrinsic collector parameters as it is suggested by the analytical relation (Eq. (1)) but also the quality of the collector ohmic contact.

IV. CONCLUSION

A calibrated 2D simulation of dc characteristics of InP/GaAsSb/InP DHBT is presented. The developed methodology has allowed to adjust some unknown or uncertain GaAsSb material parameters. In particular we found that the base bandgap is about 10% lower than the expected value. This result is attributed to a band gap narrowing due to the heavy doping and/or the polycrystalline effect. Moreover, at high injection, the current gain degradation mechanism has been investigated. We have shown that the gain drop is caused by the formation of a parasitic barrier at the base-collector interface but also depends on the quality of the collector ohmic contact.

REFERENCES

- [1] R. Bhat, W-P. Hong, C. Caneau, M. A. Koza, C-K. Nguyen, and S. Goswami, "InP/GaAsSb/InP and InP/GaAsSb/InGaAsP double heterojunction bipolar transistors with a carbon-doped base grown by organometallic chemical vapor deposition", *Appl. Phys. Lett.* Vol. 68, pp.985-987, June 1996.
- [2] B.T McDermott E. R. Gertner, S. Pittman, C. W. Seabury, and M. F. Chang, "Growth and doping of GaAsSb via metalorganic chemical vapor deposition for InP heterojunction bipolar transistor", *Appl. Phys. Lett.*, Vol. 68, pp.1386-1388, March 1996.
- [3] M. W. Dvorak, N. Matine, and C. R. Bolognesi, X. G. Xu and S. P. Watkins, "Design and performances of InP/GaAsSb/InP double heterojunction bipolar transistors", *J. Vac. Sci. Technol.*, Vol. A18, pp.761-763, March 2000.
- [4] M. W. Dvorak, C. R. Bolognesi, Watkins, "300GHz InP/GaAsSb/InP double HBTs with high current capability and $BV_{CE0} > 6\text{V}$ ", *IEEE Electron Device Letter*, Vol. 22, pp.361-363, August 2001.
- [5] R. Stratton, "Diffusion of hot electrons in semiconductor barrier", *Phys. Rev.*, Vol. 126, pp. 2002-2014, 1962.
- [6] R. E. Nahory, M. A. Pollack, J. C. DeWinter and K. M. Williams, "Growth and properties of liquid-phase epitaxial GaAsSb" *J. Appl. Phys.*, Vol.48, pp. 1607-1614, April 1977.
- [7] Gueofu Niu and John D. Cressler, "The impact of bandgap offset distribution between conduction and valence bands in Si-based graded bandgap HBT's", *Solid-State Electron*, Vol. 43, pp.2225-2230, 1999.
- [8] C. R. Bolognesi and S.P. Watkins, "Compound Semiconductor", Vol. 6, pp.94-95, 2000.
- [9] C. R. Bolognesi N. Matine, X. G. Xu, G. Soerensen and S. P. Watkins, "InP/GaAsSb/InP fully self-aligned double heterojunction bipolar transistors with a C-doped base: a preliminary reliability study", *Microelectronics Reliab.*, Vol.39, pp.1833-1838, 1999.
- [10] B. Mazhari and H. Morkoç "Effect of collector-base valence-band discontinuity on Kirk effect in double-heterojunction bipolar transistors", *Appl. Phys. Lett.*, Vol.59, pp.2162-2164, 1991.